Inorganic Chemistry

Article

pubs.acs.org/IC

Spectroscopic and Crystallographic Investigations of Novel BODIPY-Derived Metal–Organic Frameworks

Ming Li,[†,#] Yi Yao,[‡,#] Jie Ding,*[,†] Lu Liu,[†] Jianhua Qin,[†] Yaopeng Zhao,*[,‡] Hongwei Hou,*[,†] and Yaoting Fan[†]

[†]College of Chemistry and Molecular Engineering, Zhengzhou University, Henan 450001, China

[‡]State Key Laboratory of Catalysis, , Dalian Institute of Chemical Physics, Chinese Academy of Sciences, 457 Zhongshan Road, Dalian 116023, China

Supporting Information

ABSTRACT: To explore new 4,4-difluoro-4-bora-3a,4a-diaza-*s*-indacene (BODIPY)-derived metal–organic frameworks (MOFs), we employed 2,6-dicarboxyl-1,3,5,7-tetramethyl-8-phenyl-4,4-difluoroboradiazaindacene (H_2L) as a ligand to successfully synthesize five coordination polymers, namely, $\{[Zn_2(L)_2(bpp)]\cdot 2H_2O\cdot 2EtOH\}_n$ (**1**), $\{[Cd_2(L)_2(bpp)]\cdot 2H_2O\cdot EtOH\}_n$ (**2**), $\{[Cd_2(L)(bpe)_3(NO_3)_2]\cdot 2H_2O\cdot DMF\cdot EtOH\}_n$ (**3**), $\{[Cd(L)(bpe)_{0.5}(DMF)(H_2O)]\}_n$ (**4**), and $\{[Cd(L)(bpe)_{0.5}]\cdot 1.5H_2O\cdot DMF\}_n$ (**5**) (bpp = 1,3-bi(4-pyridyl)propane, bpe = 1,2-bi(4-pyridyl)ethane). Except for two 2D-layer coordination polymers **3** and **4**, the rest samples exhibit 3D metal–organic frameworks with certain pore sizes, especially MOFs **1** and **5**. Spectroscopic and crystallographic investigations demonstrate that the absorption and emission energies of the BODIPY chromophores are sensitive to the coordination modes. Moreover, in case **2**, the transition metal centers coordinated with the dicarboxylate ligands L^{2-} are capable of forming the two BODIPY units in coplanar arrangements (θ = 37.9°), simultaneously suppressing the uncommon J-dimer absorption band centered at 705 nm with a long tail into the near-infrared region at room temperature. On the other hand, in comparison with the ligand H_2L, the emission of monomer-like BODIPY in case **3** is enhanced in the solid state by a considerably long distance between the parallel BODIPY planes (about 14.0 Å).

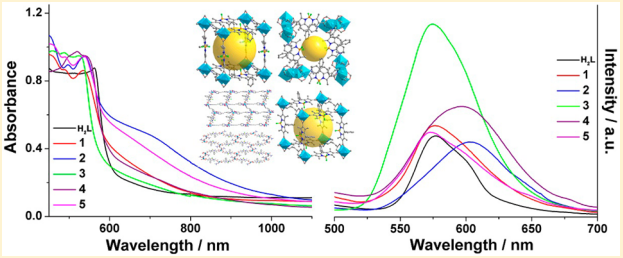

INTRODUCTION

During the past decade, metal–organic frameworks (MOFs), also called porous coordination polymers (PCPs), made by reticular synthesis with polytopic organic struts and inorganic nodes, have constituted an attractively versatile platform for achieving long-range organization and order.[1,2] Because of their easily tailored structures and exploitable properties, MOFs have been one hot subject of research in the eyes of many chemists and material scientists, which have aroused them with great enthusiasm in different areas.[3−5] In particular, the multifunctional nature of these systems was used to explore the applications in light-emitting devices,[6] light-harvester,[7] nonlinear optics,[8] photoinduced hydrogen production,[4e,9] chemical sensor,[10] and biomedicine[11] by combining optical properties with several other properties,[3a,12] such as microporosity, molecule and ion sensing, and catalysis.

4,4-Difluoro-4-bora-3a,4a-diaza-*s*-indacene (BODIPY), one kind of brilliant small molecule dye,[13] shows distinctly charming photophysical properties that include strong visible absorption, relatively sharp fluorescence with efficient quantum yield, relative insensitiveness to environment pH or polarity, and reasonable stability to physiological conditions.[14] In addition, the packing of such a dye in aggregated solid states may be engineered to facilitate the formation of J-type aggregates (head-to-tail), which exhibit large bathochromic shifts in absorption spectra relative to the monomers.[15] Significantly, because small modifications of their structures enable tuning their photophysical features, BODIPY-derived materials have been widely employed as useful tools for many different applications.[16,17] Accordingly, the attachment of BODIPY units to a transition metal center is also highly attractive, most of which are complex molecule examples.[18−22] Recently, Nitschke and co-workers have synthesized a series of emissive metallo-supramolecular cages by incorporating BODIPY fluorophores.[20] Despite the intriguing properties, the chemistry of BODIPY-derived coordination polymers has remained relatively unexplored. In 2011, Hupp and co-workers first reported two BODIPY-derived MOFs (**BOB** and **BOP**), which are capable of harvesting light across the entire visible spectrum by strut-to-strut energy transfer.[21] As followed, another two photoluminescent MOFs were obtained based on a BODIPY-derived bipyridine ligand.[22] Since such field is at an early stage of development, we are very interested in constructing new BODIPY-derived MOFs and exploring the relationship between photophysical properties and the structures in order to get a series of multifunctional materials

Received: September 14, 2014
Published: January 14, 2015

DOI: 10.1021/ic502219y
Inorg. Chem. 2015, 54, 1346−1353

Scheme 1. Synthetic Procedure for Ligand H_2L

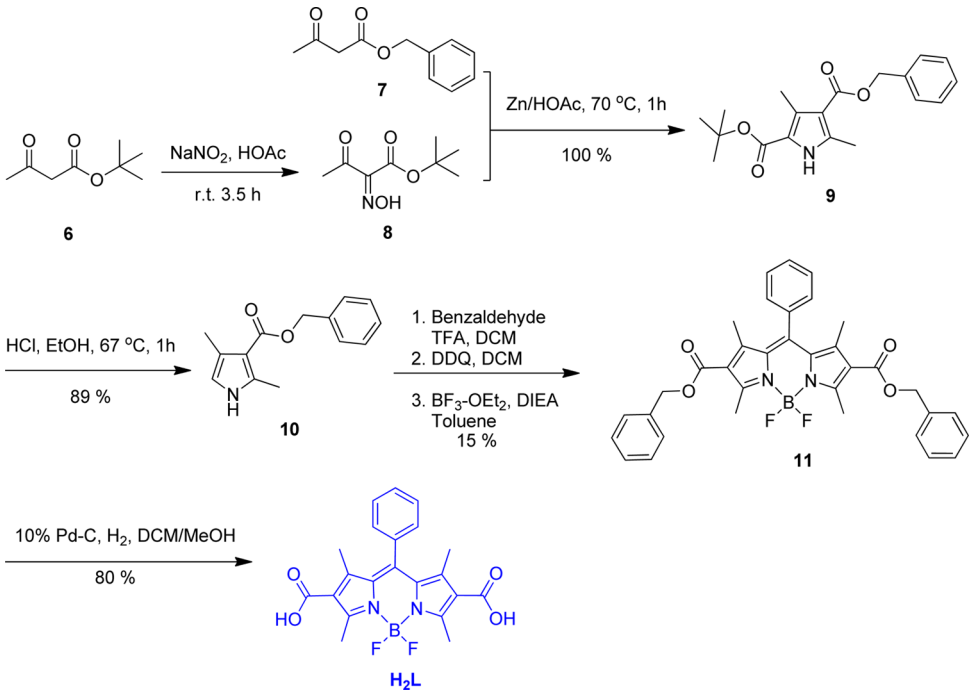

with potential applications in optoelectronics, light-harvesting, etc.

Herein, by employing 2,6-dicarboxyl-BODIPY ligand H_2L as a chromophore linker, five coordination polymers $\{[Zn_2(L)_2(bpp)]\cdot 2H_2O\cdot 2EtOH\}_n$ (**1**), $\{[Cd_2(L)_2(bpp)]\cdot 2H_2O\cdot EtOH\}_n$ (**2**), $\{[Cd_2(L)(bpe)_3(NO_3)_2]\cdot 2H_2O\cdot DMF\cdot EtOH\}_n$ (**3**), $\{[Cd(L)(bpe)_{0.5}(DMF)(H_2O)]\}_n$ (**4**), and $\{[Cd(L)(bpe)_{0.5}]\cdot 1.5H_2O\cdot DMF\}_n$ (**5**) (bpp =1,3-bi(4-pyridyl)propane, bpe = 1,2-bi(4-pyridyl)ethane) have been formulated by changing the metal ions and auxiliary pyridine ligands. Except for two 2D-layer coordination polymers **3** and **4**, the rest of the samples exhibit 3D MOFs with certain pore sizes, especially MOFs **1** and **5**. Spectroscopic investigations demonstrate that in case **2**, the uncommon J-dimer absorption band is observed at λ_{max} = 705 nm with a long tail into the near-infrared (NIR) region at room temperature. On the other hand, in comparison with the ligand H_2L, the emission of monomer-liked BODIPY in case **3** is enhanced more than twice in the solid state.

EXPERIMENTAL SECTION

Materials. All chemical reagents were purchased from commercial suppliers and used without further purification, unless otherwise indicated. Ligand H_2L was synthesized by the procedure in Scheme 1.

Physical Measurements. ^1H NMR (400 MHz) spectra were measured on a Varian infinity-plas spectrometer with TMS as the internal standard. FT-IR spectra were recorded on a Bruker-ALPHA spectrophotometer using dry KBr disks in the range of 4000−400 cm^{-1}. Elemental analyses for carbon, hydrogen, and nitrogen were carried out on a FLASH EA 1112 analyzer. Thermogravimetric analyses (TGA) were implemented on a Netzsch STA 449C thermal analyzer, and the samples were heated at a rate of 10 °C min^{-1} under the air atmosphere. The room-temperature powder X-ray diffraction spectra were performed on a PANalytical X'Pert PRO diffractometer using Cu Kα1 radiation. UV−vis absorption spectra in the solid state were measured from 200 to 1100 nm by a Cary 5000 spectrophotometer equipped with a 110 nm diameter integrating sphere. The measurements of steady-state emission spectra in the solid state were conducted on a Hitachi 850 fluorescence spectrophotometer at room temperature. The quantum yield of sample emission in the solid state was detected with an absolute photoluminescence quantum yield measurement system (C11347-11, Hamamatsu Photonics) under excitation at 450 nm at room temperature. The gas sorption isotherms of coordination polymers **1** and **5** were collected on a Micromeritics 3Flex surface area and pore size analyzer under ultrahigh vacuum in a clean system, with a diaphragm and turbo pumping system. Ultrahigh-purity-grade (>99.999%) N_2 gas was applied in all adsorption measurements. The experimental temperature was maintained by liquid nitrogen (77 K). Prior to measurement, to remove the solvent molecules, the bulk samples of complexes **1** and **5** were soaked in acetone for 2 days with the solvent refreshed every 12 h and then dried in a vacuum oven at 60 °C for 12 h. Moreover, supercritical CO_2 (SC−CO_2) activation also was used to remove the solvent molecules in sample **1** by a custom-built system. Typically, a bulk sample of complex **1** was washed by absolute ethanol (EtOH) three times, dried under a vacuum, and then transferred into a stainless steel column. After 20 min of soaking and venting of supercritical CO_2 by a DB-80 simplex pump, the column pressure regulator was set at 100 bar by soaking SC−CO_2, and the column temperature was raised to 55 °C. SC−CO_2 in the column was gradually vented after 14 h. The activation samples were placed in sealed containers for nitrogen adsorption. TGA experiments and powder X-ray diffraction were carried out to make sure that the solvent molecules were removed completely and the framework structures retained crystallinity after activation, respectively.

Syntheses. *tert-Butyl 2-Hydroximino-3-oxobutyrate (**8**).* *tert*-Butyl 3-oxobutanoate (**6**, 40 mL, 241 mmol) was dissolved in acetic acid (80 mL) in a round-bottomed flask, and the mixture was cooled in an ice bath to about 10 °C. Sodium nitrite (18 g, 261 mmol) was added over 1 h while the temperature was kept under 15 °C. The cold bath was removed, and the mixture was allowed to stir for 3.5 h at room temperature to give a crude solution of **8** which was used in the next step without further purification.

*3, 5-Dimethyl-1H-pyrrole-2, 4-dicarboxylic Acid 2-tert-Butyl Ester 4-Benzyl Ester (**9**).* To a stirred mixture of benzyl 3-oxobutyrate (**7**, 13.7 mL, 79 mmol) and acetic acid (100 mL) in an oil bath, zinc dust (50 g, 0.76 mol) was added portionwise. The mixture was heated to 60 °C. At this temperature, the crude **8** precipitated slowly. The temperature was then increased to 75 °C for 1 h, and then the

DOI: 10.1021/ic502219y
Inorg. Chem. 2015, 54, 1346−1353

reaction mixture was poured into water (40 mL). The precipitate was collected by filtration to yield **9** in quantitative yield as a white solid. ^{1}H NMR (400 MHz, $CDCl_3$): 8.88 (br, s, 1H, NH), 7.47−7.33 (m, 5H, C═CH), 5.29 (s, 2H, CH_2), 2.53, 2.48 (2s, 6H, $2CH_3$), 1.56 (s, 9H, $3CH_3$).

*2,4-Dimethyl-1H-pyrrole-3-carboxylic Acid Ester (**10**).* A solution of the product **9** (22.07 g, 67 mmol) dissolved in ethanol (78 mL) was stirred vigorously as hydrochloric acid (10 N, 3.6 mL) was slowly added at 20 °C. Then the reaction mixture was heated to 67 °C for 1 h, cooled to 5 °C, and poured into ice water. The solid was collected by filtration and washed with water to yield 2, 4-dimethyl-1H-pyrrole-3-carboxylic acid ester (8.10 g, 89% yield). ^{1}H NMR (400 MHz, $CDCl_3$): 10.48 (br, s, 1H, NH), 7.47−7.33 (m, 5H, C═CH), 6.35 (s, 1H, CH), 4.10 (q, 2H, CH_2), 2.35, 2.15 (2s, $2CH_3$).

*2,6-diCO_2Bzl-BDP (**11**).* The synthetic procedure is according to the literature.[23] ^{1}H NMR (400 MHz, $CDCl_3$): 7.49 (m, 3H, C═CH), 7.3−7.4 (m, 10H, C═CH), 7.22 (m, 2H, C═CH), 5.22 (s, 4H, $2CH_2$), 2.82 (s, 6H, $2CH_3$), 1.58 (s, 6H, $2CH_3$).

*2,6-diCO_2H-BDP (**H_2L**).* The synthetic procedure is according to the literature.[23] ^{1}H NMR (400 MHz, DMSO-d_6): 12.73 (s, 2H, COOH), 7.56 (m, 3H, C═CH), 7.40 (m, 2H, C═CH), 2.68 (s, 6H, $2CH_3$), 1.55 (s, 6H, $2CH_3$).

*{[Zn_2(L)$_2$(bpp)]·2H_2O·2EtOH}$_n$ (**1**).* A mixture of H_2L (8.2 mg, 0.020 mmol), bpp (9.9 mg, 0.05 mmol), $Zn(NO_3)_2·6H_2O$ (14.9 mg, 0.05 mmol), DMF (2 mL), and an aliquot of HNO_3 in EtOH (4 mL of a 0.03 M solution) was sealed in the autoclave at 80 °C for 2 days and then cooled to room temperature. Orange-red crystals of **1** were collected in a ca. 60% yield based on H_2L ligand. Elemental analysis for $C_{59}H_{64}B_2F_4N_6O_{12}Zn_2$, calcd (%): C, 55.47; H, 5.05; N, 6.58. Found (%): C, 55.51; H, 5.01; N, 6.49. IR data (KBr, ν/cm^{-1}): 3435 (m), 2927 (w), 1621 (w), 1534 (m), 1430 (m), 1401 (w), 1343 (s), 1313 (m), 1144(s), 1072 (m), 1024 (s), 811 (m), 727 (m), 669 (w), 599(m).

*{[Cd_2(L)$_2$(bpp)]·2H_2O·EtOH}$_n$ (**2**).* Dark red petal-shaped crystals of **2** were obtained using the same method as that for **1**. The reagents used were H_2L (8.2 mg, 0.020 mmol), bpp (4.0 mg, 0.02 mmol), $Cd(NO_3)_2·4H_2O$ (15.4 mg, 0.05 mmol). Yield: 45% based on H_2L ligand. Elemental analysis for $C_{57}H_{58}B_2Cd_2F_4N_6O_{11}$, calcd (%): C, 51.65; H, 4.41; N, 6.34. Found (%): C, 51.59; H, 4.50; N, 6.28. IR (KBr, ν/cm^{-1}): 3430 (m), 2925 (m), 1617 (w), 1615 (w), 1532 (s), 1428 (m), 1399 (m), 1342 (s), 1312 (m), 1190 (s), 1142 (s), 1071 (m), 1022 (s), 822 (m), 785 (w), 727 (m), 667 (w), 598 (m), 572 (m).

*{[Cd_2(L)(bpe)$_3$(NO_3)$_2$]·2H_2O·DMF·EtOH} (**3**).* A mixture of H_2L (8.2 mg, 0.020 mmol), bpe (9.2 mg, 0.05 mmol), $Cd(NO_3)_2·4H_2O$ (15.4 mg, 0.05 mmol), DMF (2 mL), and an aliquot of HNO_3 in EtOH (4 mL of a 0.03 M solution) was sealed in the autoclave at 80 °C for 2 days and then cooled to room temperature. Orange-red lamellar crystals of **3** were obtained. Yield: 45% based on H_2L ligand. Elem. Anal. Calcd (Found) for $C_{62}H_{70}BCd_2F_2N_{11}O_{14}$: C, 50.76 (50.82); H, 4.81 (4.74); N, 10.50 (10.45). IR (KBr, ν/cm^{-1}): 3422 (m), 2929 (w), 1655 (s), 1586 (w), 1539 (s), 1422 (m), 1397 (m), 1336 (s), 1312(m), 1258 (w), 1192 (s), 1142 (s), 1106 (w), 1074(m), 1022(m), 830 (w), 817 (m), 598 (m), 582 (m), 548 (m).

*{[Cd(L)(bpe)$_{0.5}$(DMF)(H_2O)]} (**4**).* Red blocklike crystals of **4** were obtained using the same method as that for **3**, except DMF and EtOH in a volume ratio of 1:1. Yield: 75% based on H_2L ligand. Elem. Anal. Calcd (Found) for $C_{30}H_{32}BCdF_2N_4O_6$: C, 51.05 (50.97); H, 4.57 (4.45); N, 7.94 (8.05). IR (KBr, ν/cm^{-1}): 3440 (s), 2926 (w), 2169 (w), 1655 (m), 1534 (m), 1428 (m), 1384 (m), 1341 (s), 1311 (m), 1189 (s), 1142 (m), 1070 (m), 1020 (m), 809 (m), 785 (w), 727 (m), 664 (w), 597 (m), 571 (w).

*{[Cd(L)(bpe)$_{0.5}$]·1.5H_2O·DMF}$_n$ (**5**).* By adopting the preparative method of **3**, except at 100 °C for 2 days and then cooled to room temperature, dark red block-shaped crystals of **5** were collected in a ca. 35% yield based on H_2L ligand. Elem. Anal. Calcd (Found) for $C_{30}H_{33}BCdF_2N_4O_{6.5}$: C, 50.41 (50.37); H, 4.65 (4.74); N, 7.83 (7.75). IR (KBr, ν/cm^{-1}): 3442 (m), 3057 (w), 2927 (m), 1676 (s), 1612 (s), 1533 (m), 1506 (w), 1429 (m), 1385 (m), 1342 (s), 1311 (m), 1285 (w), 1190 (s), 1144 (m), 1072 (m), 1017 (s), 827 (s), 728 (m), 598 (m), 577 (m).

Crystal Data Collection and Refinement. Single crystal X-ray diffraction analyses of complexes **1** and **2** were carried out on a SuperNova diffractometer with graphite monochromated Cu Kα radiation (λ = 1.54178 Å) at 100(2) K, whereas the data of complexes **3**−**5** were collected on a Rigaku Saturn 724 CCD diffractometer with Mo Kα radiation (λ = 0.71073 Å) at 20 ± 1 °C. The empirical absorption corrections were applied by the multiscan program. The crystal data were corrected for Lorentz and polarization effects. The structures were solved by direct methods and then refined for non-hydrogen atoms by full-matrix least-squares techniques on the basis of F^2 using the SHELXL-97 program.[24] There were large solvent accessible pore volumes in complexes **1**, **2**, and **5**, occupied by highly disorded solvent molecules as well as those of complex **3**. No satisfactory disorder model could be achieved, and therefore the SQUEEZE program implemented in PLATON was used to remove these electron densities. The numbers of guest molecules for **1**, **2**, **3**, and **5** were calculated by the TGA and elemental analysis data. Crystallographic processing parameter and selected bond lengths and bond angles for **1**−**5** are listed in Tables S1 and S2 (in the Supporting Information), respectively. Crystallographic data for **1**−**5** have been deposited at the Cambridge Crystallographic Data Centre with CCDC reference numbers 1023699−1023703.

RESULTS AND DISCUSSION

Synthetic Aspect. As we know, the luminescence was often ascribed to the π-conjugated organic linker in many MOFs, such as dicarboxylate-containing species. Because of the excellent luminescent property of the BODIPY-based dicarboxylic acid H_2L in solution,[23] it would be a novel platform to construct functional high-dimensional coordination compounds. As shown in Scheme 1, the chromophore linker, H_2L was synthesized by a simplified procedure compared to the reported literature.[23] At first, screening for simple and cheap precursor **6** as the starting material, intermediate product **9** was synthesized by the fast one-step cyclization reaction with very high yield. Subsequently, complex **10** was obtained by 1 h elimination reaction. Significantly, in comparison with the reported procedure,[23] this synthetic process was not only with higher yield but also needed much less reaction time and softer chemical condition.

Crystal Structure and Characterization. Five coordination polymers **1**−**5** were successfully obtained by the solvothermal reactions with the chromophore linker H_2L, metal salts ($M(NO_3)_2$, M = Zn/Cd) and auxiliary pyridine ligands (bpp and bpe) in DMF and HNO_3 in ethanol media, respectively. Single crystal X-ray diffraction analyses present all the structures of coordination polymers **1**−**5**, which are further confirmed by the powder X-ray diffraction (PXRD), thermogravimetric analyses (TGA), elemental analyses, and infrared (IR) spectroscopy experiments.

In case **1**, the single crystal X-ray diffraction pattern demonstrates a 3D pillared-layer framework, which belongs to the monoclinic system with $C2/c$ space group. As shown in Figures 1a and S1, two adjacent Zn ions, bridged by the carboxylate groups of BODIPY-based ligands, form a paddle-wheel type secondary building unit (SBU)−[$Zn_2(COO)_4$] with Zn−Zn distance about 3.0 Å, which is connected by four BODIPY-based dicarboxylic acid groups and further extended into a 2D sheet-like layer. At the same time, these 2D layers are pillared by the bpp linkers along the c axis to give rise to a 3D pillared-layer porous framework with pore sizes of ∼14.8 × 14.8 Å^2, while the structure induces 2-fold interpenetration of the framework which reduces the void space with pore sizes of

DOI: 10.1021/ic502219y
Inorg. Chem. 2015, 54, 1346−1353

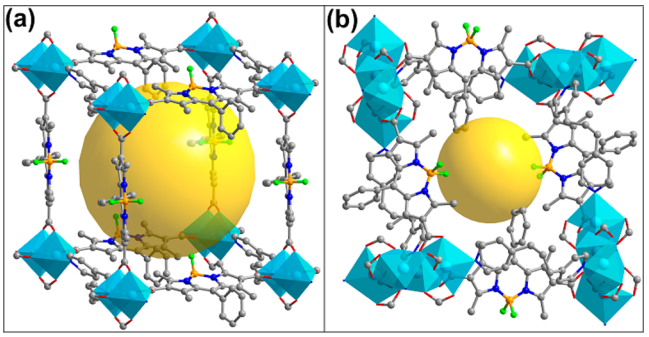

Figure 1. Schematic representation of the structures of complexes **1** (a) and **2** (b). Hydrogen atoms and solvent molecules have been omitted for clarity.

~11.5 × 11.5 Å^2. Therefore, MOF **1** can be represented as a 6-connected 2-fold interpenetration topology, and the point symbol for the net is $4^{12}\cdot6^3$. A PXRD experiment for case **1** also has been carried out to check its phase purity. As shown in Figure S2, the peak positions of the experimental PXRD spectrum match well with that of th esimulated one, indicating that the crystal structure is truly representative of the bulk sample. The differences in intensity may be due to the preferred orientation of the crystal products. In addition, application of the SQUEEZE routine in PLATON suggests that a void volume is 35% in the total cell. These channels are occupied by H_2O and EtOH, which are confirmed by elemental analysis and TGA. Furthermore, a TGA experiment was performed under air atmosphere to check the thermal stability of MOF **1** (Figure S3). For instance, it successively lost weight of 10.05% (calcd 10.03%) in the range of 30−277 °C due to one lattice water molecule and one EtOH molecule, which also implies the porosity. Over 277 °C, the framework of sample **1** was unstable and decomposed gradually. Thus, gas sorption measurement for the as-synthesized sample **1** after acetone exchange was conducted up to a relative pressure (p/p_0) of 1.0 on the activated frameworks at STP. N_2 adsorption isotherm demonstrates that MOF **1** exhibits a small gas adsorption value of 18 cm^3/g with a Brunauer−Emmett−Teller (BET) surface area of 27 m^2/g (Figure S4). This result may be attributed to the change from crystalline phase to amorphous phase of MOF **1**, on account of the broadening, or even disappearing of some peaks in the PXRD spectrum (Figure S2).[22] Furthermore, the flowing SC−CO_2 activation also has been used to avoid collapse during volatile solvent evacuation.[28] After SC−CO_2 activation, as shown in Figure S4, the N_2 adsorption isotherm of MOF **1** illustrates the BET surface area of 257 m^2/g with the gas adsorption value of 121 cm^3/g.

Surprisingly, by the same solvothermal method except changing metal salts into $Cd(NO_3)_2\cdot4H_2O$, coordination polymer **2** features a totally different 3D framework, which can be simplified into a 8-connected topology with the point symbol $4^{24}\cdot6^4$ (Figures 1b and S5). Two carboxylic groups of BODIPY-based ligands both adopt μ_2-η^2:η^1-chelate/bridge coordination fashions, which link Cd(II) ions to provide a tetranuclear SBU− $[Cd_4(CO_2)_8]$. Each tetranuclear SBU is surrounded by eight L^{2-} units and further furnish a complicated 3D MOF, while the bpp ligand just plays a role in connecting Cd(II) ions from two adjacent SBUs to add the linking numbers of the tetranuclear SBUs. Hence, a void volume of 22% in the total cell was indicated by the SQUEEZE routine in PLATON. In case **2**, the experimental PXRD data also displayed that the crystal structure was totally representative of the bulk sample (Figure S6). Moreover, TGA experiment showed that coordination polymer **2** lost two lattice water molecules and one EtOH molecule (obsd 6.05%, calcd 6.19%, Figure S7) when the temperature was raised from 30 to 254 °C. In addition, the resultant structure was stable up to 306 °C and finally decomposed to CdO.

In consideration of interpenetration in MOF **1**, we tried to reduce the flexibility of pyridine ligand to construct 3D MOF probably containing larger porosity. Surprisingly, when the bpe linker was used instead of the bpp group, two 2D-layer coordination polymers **3** and **4** were obtained by the similar solvothermal method (Figure 2a,b). For coordination polymer

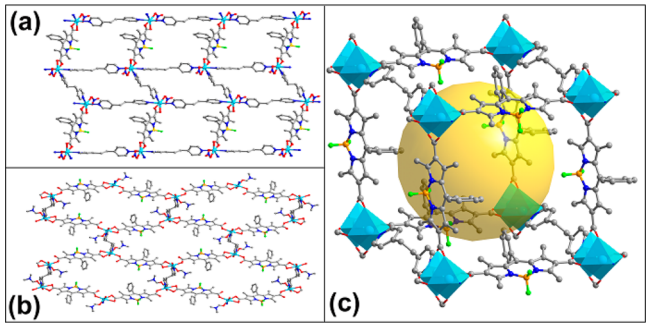

Figure 2. Schematic representation of the structures of complexes **3** (a), **4** (b) and **5** (c). Hydrogen atoms and solvent molecules were omitted for clarity.

3, as shown in Figures S8 and 2a, the bpe groups connect Cd(II) ions to form a 1D ladder-shape chain, and subsequently, linked by BODIPY-based dicarboxylic acids in chelated coordination modes, the chains are extended into a 2D wave-like layer. Complex **3** illustrated very high phase purity detected by the PXRD experiment (Figure S9). In contrast, while the volume ratio of reaction solvent DMF/EtOH was turned into 1:1, the two carboxylic groups of ligand L^{2-} adopt μ_1-η^1:η^1 and μ_1-η^0:η^1 coordination modes in complex **4** (Figures S10 and 2b), respectively, which provide a 1D infinite chain by linking Cd(II) ions. Interestingly, bridged by the bpe groups, the 1D chains further form a graphene-like 2D layer. In each hexagonal circle unit of such 2D layer, six Cd(II) ions are like the "C atoms", which are linked by four BODIPY-based dicarboxylic acids and two bpe moieties. The experimental PXRD data also exhibited that the crystal structure of complex **4** was totally representative of the bulk sample (Figure S11). As shown in Figure S7, from 90 to 230 °C, complex **3** lost two lattice water molecules, one EtOH and one DMF (obsd 10.50%, calcd 10.58%) and became unstable beyond 260 °C. In comparison with that of case **3**, the thermal stability of coordination polymer **4** was better, which lost one coordinated water molecule and one coordinated DMF molecule in the scale of 90−330 °C (obsd 12.60%, calcd 12.91%), and above 330 °C, complex **4** decomposed continuously until 800 °C.

Ultimately, under the same solvothermal reaction condition except for raising the reaction temperature to 100 °C, a 3D pillared-layer framework **5** was successfully synthesized, which was the isoreticular framework of complex **1** deliberated by the crystallographic analysis (Figure 2c). For instance, ligands L^{2-} chelate Cd1 ion and symmertry-related Cd1A ion to form a $[Cd_2(CO_2)_4]$ binuclear SBU with Cd−Cd distance about 3.04 Å, which further gives rise to a 2D layer (Figure S12).

DOI: 10.1021/ic502219y
Inorg. Chem. 2015, 54, 1346−1353

Furthermore, the 2D networks are sustained by the bpe moieties along the *c* direction to generate a pillared-layer 3D framework. Structural topology analysis reveals that $4^{12}\cdot6^3$ is the point symbol for this net. As a result of 2-fold interpenetration with real pore sizes of ~11.3 × 11.3 Å^2, calculation by using PLATON suggests the guest accessible void comprises 40% of the total cell volume. Although complexes **1** and **5** are isoreticular, the distances of two adjacent binuclear SBUs bridged by pyridine ligands bpp or bpe in complexes **1** and **5** are 16.0286 and 16.675 Å, respectively, which may be attributed to differences of the pillar molecules (bpp for complex **1** and bpe for complex **5**) and metal nodes (Zn for complex **1** and Cd for complex **5**). As shown in Figure S13, because the data of the experimental PXRD spectrum is consistent with that of simulated one, the crystal structure of **5** completely expressed the bulk sample. For MOF **5**, a weight loss of 14.33% in 20−245 °C range was consistent with the removal of one DMF and one and a half lattice water molecules (calcd 14.00%, Figure S14), and the dehydrated compound was stable to 308 °C. To consider the results of crystallographic analysis and TGA measurement, 1D channels with considerable void spaces are present in MOF **5**. As shown in Figure S15, sample **5** shows a type-I behavior in N_2 adsorption isotherm at 77 K, which indicates a gas uptake of 60 cm^3/g with the BET surface area of 138 m^2/g.

Photophysical Properties. Before the detailed spectroscopic investigations of the coordination polymers **1**−**5**, macroscopic images of **1**−**5** under natural light and 365 nm UV irradiation would roughly manifest some photophysics information. As shown in inset images of Figure 3, case **2** exhibits the much deeper color comparing to the rest of the as-synthesized samples and red ligand H_2L (Figure S16), indicating that the energy of $S_0 \rightarrow S_1$ transition in **2** is probably lower than those of the rest of the samples (**1**, **3**, **4**, and **5**) and ligand H_2L. On the other hand, under irradiation of 365 nm UV light, all the samples show orange or red photoluminescence with the naked eyes.

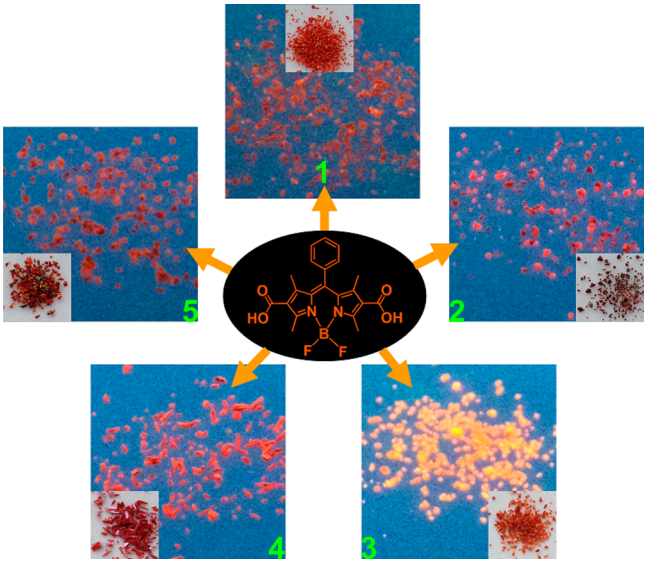

Figure 3. Macroscopic images of coordination polymers **1**−**5** under 365 nm UV irradiation; inset: macroscopic images of the corresponding crystals under natural light, respectively.

In this work, the UV−vis absorption spectra of ligand H_2L, bpe, bpp, and the coordination polymers **1**−**5** were recorded in the solid state at room temperature (Table 1, Figure S17). As depicted in Figure 4a, ligand H_2L exhibits several intense absorption bands in the range of 210−570 nm. At the same time, careful inspection of the spectrum on the low-energy side reveals a small peak in the region of 600−800 nm. This could indicate a weak transition centered at around 651 nm (15 360 cm^{-1}) within the tail. The intense absorption band is at λ_{max} = 562 nm (17795 cm^{-1}), which is ascribed to the $\pi \rightarrow \pi^*$ transition of the monomer-like BODIPY group, while the weak band in lower energy range is possibly the transition of J-aggregates based on dipole−dipole interaction in the aggregate.[23,25] Furthermore, the lowest energy absorption band of ligand bpp or bpe is at λ < 285 nm (35090 cm^{-1}, Figure S17), which is distinctly higher than that of ligand H_2L in the energy level. As a result, the BODIPY group of ligand H_2L will play a key role as the chromophore after being coordinated with the Zn(II)/Cd(II) metal ions.

Table 1. Absorption and Steady-State Fluorescence Properties of Crystals 1−5 and Ligand bpe, bpp, and H_2L in Power State at Room Temperature

sample	λ_{ab}/nm	λ_{em}/nm	$\Delta\upsilon_{St}$[c]/cm^{-1}	ϕ_F[d]
1	212, 256, 354−391,[a] 448, 489, 535, 658	577	1360	0.0082
2	213, 254, 344−392,[a] 447, 497, 539, 705	602	1942	0.0067
3	211, 257, 346−389,[a] 458, 487, 524	574	1662	0.017
4	210, 264, 344−395,[a] 495, 520, 540, 654	596	1740	0.0099
5	210, 263, 341−393,[a] 447, 489, 537, 677	573	1170	0.0076
bpe	210, 249, 282	*b*	*b*	*b*
bpp	210, 249, 274	*b*	*b*	*b*
H_2L	213, 263, 373, 409, 562, 651	577	465	0.0073

[a]Broad signal including multipeaks. [b]Not measured in this paper. [c]Stokes shift = $(1/\lambda_{ab} - 1/\lambda_{fl})$. [d]Quantum yield was measured with an absolute photoluminescence quantum yield measurement system (C11347-11, Hamamatsu Photonics) upon excitation at 450 nm.

Remarkably, compared to that of ligand H_2L, the $\pi \rightarrow \pi^*$ transition of the monomer-like BODIPY group is visibly blue-shifted in each of the samples **1**−**5** (Table 1, **1**: 535 nm, **2**: 539 nm, **3**: 524 nm, **4**: 540 nm, and **5**: 537 nm), which might result from the increasing electron-withdrawing character of carboxylate groups at the 2,6-positions by being coordinated with the transition metal ions.[23] In addition, in comparison with the inferred transition of powder sample H_2L in lower energy level, the relative intensity are enhanced in the coordination polymers except for sample **3**. Especially in case **2**, such absorption band grows into a strong shoulder peak centered at 705 nm (14 185 cm^{-1}) with a long tail into the near-infrared (NIR) region. However, in case **3**, such estimated dimer transition disappeared as shown in Figure 4a. As we know, BODIPY groups in J aggregates are arranged in a head-to-tail direction or coplanar displacements with θ < 54.7°. Only the transition to the lowest excited state is allowed, which is characterized by a bathochromic shift of the absorption maximum compared to the monomer.[26] As exhibited in Figure 5a, the BODIPY moieties in complex **2** can be arranged in coplanar displacements with θ = 37.9°, and the center distance between the BODIPYs is about 5.7 Å measured by the crystallographic

DOI: 10.1021/ic502219y
Inorg. Chem. 2015, 54, 1346−1353

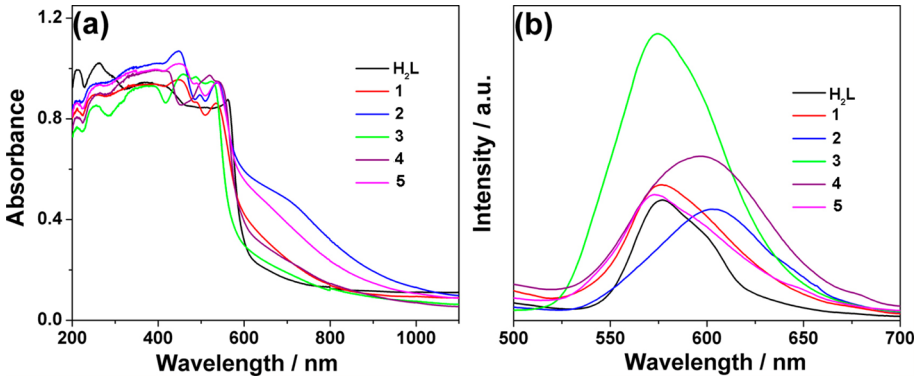

Figure 4. (a, b) Diffuse-reflectance UV−vis and fluorescence spectra of ligand H_2L and complexes **1**−**5** in the solid state at room temperature (λ_{ex} = 450 nm, the emission intensity in panel b corresponds to the result of absolute photoluminescence quantum yield measurement).

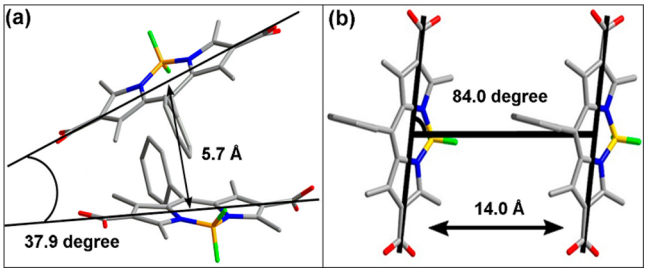

Figure 5. Partial packing diagrams of the BODIPY units in sample **2** (a) and **3** (b), respectively. H atoms are omitted for clarity.

analysis. Hence, in case **2**, such absorption band centered at 705 nm is clearly assigned by the transition of J-dimer based on dipole−dipole interaction.

Furthermore, to prove the hypothesis for the evidence in absorption spectroscopic measurement, some information was observed in the luminescence studies of the ligand H_2L and as-synthesized coordination polymers **1**−**5**. The room temperature emission spectra of the ligand H_2L and samples **1**−**5** in the solid state are shown in Figure 4b. Upon excitation at λ > 590 nm, ligand H_2L has no emission observed, although such $S_0 \rightarrow S_1$ transition would result in a potential luminescence in the NIR, as the associated long radiative lifetime of the corresponding emission is easily quenched by the surrounding environment in solid state or suffered by the self-quenching due to the high concentration. Interestingly, upon excitation at 450 nm, it exhibited an emission at λ_{max} = 577 nm (17330 cm^{-1}) at room temperature with a small absolute quantum yield of 0.0073. Moreover, due to the small Stokes shift of 465 cm^{-1} (Table 1), this fluorescence is derived from the $^1\pi\pi^*$ excited state of the monomer-like BODIPY group in nature.

Similar to ligand H_2L, there are also no emissions in the spectra of complexes **1**, **2**, **4**, and **5** upon excitation at 600 nm. In contrast, upon excitation at λ > 430 nm, complexes **1**−**5** still display the emissions assigned to the $^1\pi\pi^*$ excited state of BODIPY group (**1**: 577 nm, **2**: 602 nm, **3**: 574 nm, **4**: 596 nm, and **5**: 573 nm), although in cases **2** and **4**, the emission bands are distinctly red-shifted. As shown in Table 1, the quite large Stokes shifts in complexes **1**−**5** (1170−1942 cm^{-1}) comparing to the ligand H_2L suggest a geometrical rearrangement between the ground and excited states,[27] which may be explained by the influence of the coordinated transition metal ions. Significantly, the emission quantum yield is increased more than twice in complex **3** (ϕ_F = 0.017). This result is in accordance with the absorption study, which is further proved by the partial packing diagrams of the BODIPY units in **3** (Figure 5b). Herein, the BODIPY units in complex **3** adopt parallel arrangements of the transition dipoles with the slip angle of θ = 84°, and the measured distance between the BODIPY-planes is about 14.0 Å. In such rigid frameworks, the BODIPY moieties could not be allowed to form the dimers and also the concentration quenching of fluorescent dyes was hindered by the considerably long distance between the BODIPY-planes in the solid state. Normally, the emission of monomer-liked BODIPY in case **3** will be enhanced.

CONCLUSIONS

As a consequence, by using BODIPY-based dicarboxylic acid H_2L as a chromophore linker, five coordination polymers **1**−**5** were successfully obtained by the solvothermal reactions with moderate-to-good yields in this work. By the metal center Cd(II) instead of Zn(II), the 3D pillared-layer framework **1** was replaced by a more compact coordination polymer **2**, which featured a totally different 3D framework with the point symbol $4^{24}\cdot6^4$. As the bpe linker instead of the bpp group reduces the flexibility of pyridine ligand, two unanticipated 2D-layer coordination polymers **3** and **4** were obtained, whereas 3D pillared-layer framework **5** was prepared with larger porosity by raising the reaction temperature at 100 °C. The combination of spectroscopic investigation and crystallographic analysis demonstrates that the absorption band of J-dimer can be observed at λ_{max} = 705 nm in the solid state since the BODIPY moieties in complex **2** are arranged in coplanar displacements with θ = 37.9°. Furthermore, in comparison with the ligand H_2L, the emission of monomer-liked BODIPY in case **3** was enhanced in the solid state, because the BODIPY moieties could not be allowed to form the dimers, and also the concentration quenching of fluorescent dyes was hindered by considerably long distance between the parallel BODIPY-planes. These results imply that, due to this BODIPY-based dicarboxylic acid H_2L as the novel chromophore linker, our study opens up interest in this new platform to construct excellently luminescent BODIPY-derived MOFs for exploring applications in optoelectronics and light-harvesting.

ASSOCIATED CONTENT

Supporting Information

Details of crystal structures, TGA, and PXRD experiments of **1**−**5**, the gas sorption measurements of **1** and **5**, the macroscopic image of H_2L and the diffuse-reflectance UV−vis

DOI: 10.1021/ic502219y
Inorg. Chem. 2015, 54, 1346−1353

spectra of ligand bpe and bpp This material is available free of charge via the Internet at http://pubs.acs.org.

AUTHOR INFORMATION

Corresponding Authors

*(J.D.) E-mail: jieding@zzu.edu.cn.
*(Y.Z.) E-mail: ypzhao@dicp.ac.cn.
*(H.H.) E-mail: houhongw@zzu.edu.cn. Fax: (86)371-67761744.

Author Contributions

#(M.L., Y.Y.) The authors contributed equally to the work and should be considered co-first authors.

Notes

The authors declare no competing financial interest.

ACKNOWLEDGMENTS

This work was financially supported by the National Natural Science Foundation (Nos. 21371155 and 21301157) and Research Found for the Doctoral Program of Higher Education of China (20124101110002).

REFERENCES

(1) (a) Yaghi, O. M.; Li, G. M.; Li, H. L. *Nature* **1995**, *378*, 703−706. (b) Venkataraman, D.; Gardner, G. B.; Lee, S.; Moore, J. S. *J. Am. Chem. Soc.* **1995**, *117*, 11600−11601. (c) Kondo, M.; Yoshitomi, T.; Seki, K.; Matsuzaka, H.; Kitagawa, S. *Angew. Chem., Int. Ed. Engl.* **1997**, *36*, 1725−1727. (d) Kitagawa, S.; Kitaura, R.; Noro, S.-I. *Angew. Chem., Int. Ed.* **2004**, *43*, 2334−2375. (e) Rowsell, J. L. C.; Yaghi, O. M. *Microporous Mesoporous Mater.* **2004**, *73*, 3−14. (f) Long, J. R.; Yaghi, O. M. *Chem. Soc. Rev.* **2009**, *38*, 1213−1214.

(2) (a) Paz, F. A. A.; Klinowski, J.; Vilela, S. M. F.; Tomé, J. P. C.; Cavaleiro, J. A. S.; Rocha, J. *Chem. Soc. Rev.* **2012**, *41*, 1088−1110. (b) Furukawa, H.; Cordova, K. E.; O'Keeffe, M.; Yaghi, O. M. *Science* **2013**, *341*, 1230444. (c) Cook, T. R.; Zheng, Y.-R.; Stang, P. J. *Chem. Rev.* **2013**, *113*, 734−777. (d) Lu, W. G.; Wei, Z. W.; Gu, Z.-Y.; Liu, T.-F.; Park, J.; Park, J.; Tian, J.; Zhang, M. W.; Zhang, Q.; Gentle, T. III; Bosch, M.; Zhou, H.-C. *Chem. Soc. Rev.* **2014**, *43*, 5561−5593. (e) Lin, Z.-J.; Lü, J.; Hong, M. C.; Cao, R. *Chem. Soc. Rev.* **2014**, *43*, 5867−5895.

(3) (a) Allendorf, M. D.; Bauer, C. A.; Bhakta, R. K.; Houk, R. J. T. *Chem. Soc. Rev.* **2009**, *38*, 1330−1352. (b) Lee, J. Y.; Farha, O. K.; Roberts, J.; Scheidt, K. A.; Nguyen, S. B. T.; Hupp, J. T. *Chem. Soc. Rev.* **2009**, *38*, 1450−1459. (c) Shekhah, O.; Liu, J.; Fischerb, R. A.; Wöll, C. *Chem. Soc. Rev.* **2011**, *40*, 1081−1106. (d) Kreno, L. E.; Leong, K.; Farha, O. K.; Allendorf, M.; Duyne, R. P. V.; Hupp, J. T. *Chem. Rev.* **2012**, *112*, 1105−1125. (e) Sumida, K.; Rogow, D. L.; Mason, J. A.; McDonald, T. M.; Bloch, E. D.; Herm, Z. R.; Bae, T.-H.; Long, J. R. *Chem. Rev.* **2012**, *112*, 724−781. (f) Horcajada, P.; Gref, R.; Baati, T.; Allan, P. K.; Maurin, G.; Couvreur, P.; Férey, G.; Morris, R. E.; Serre, C. *Chem. Rev.* **2012**, *112*, 1232−1268. (g) Makal, T. A.; Li, J.-R.; Lu, W. G.; Zhou, H.-C. *Chem. Soc. Rev.* **2012**, *41*, 7761−7779. (h) Liu, J. W.; Chen, L. F.; Cui, H.; Zhang, J. Y.; Zhang, L.; Su, C.-Y. *Chem. Soc. Rev.* **2014**, *43*, 6011−6061.

(4) (a) Hu, A. G.; Ngo, H. L.; Lin, W. B. *J. Am. Chem. Soc.* **2003**, *125*, 11490−11491. (b) Alkordi, M. H.; Liu, Y. L.; Larsen, R. W.; Eubank, J. F.; Eddaoudi, M. *J. Am. Chem. Soc.* **2008**, *130*, 12639−12641. (c) Allendorf, M. D.; Houk, R. J. T.; Andruszkiewicz, L.; Talin, A. A.; Pikarsky, J.; Choudhury, A.; Gall, K. A.; Hesketh, P. J. *J. Am. Chem. Soc.* **2008**, *130*, 14404−14405. (d) Furukawa, H.; Yaghi, O. M. *J. Am. Chem. Soc.* **2009**, *131*, 8875−8883. (e) Dan-Hardi, M.; Serre, C.; Frot, T.; Rozes, L.; Maurin, G.; Sanchez, C.; Férey, G. *J. Am. Chem. Soc.* **2009**, *131*, 10857−10859. (f) Gascon, J.; Kapteijn, F. *Angew. Chem., Int. Ed.* **2010**, *49*, 1530−1532. (g) McKinlay, A. C.; Morris, R. E.; Horcajada, P.; Férey, G.; Gref, R.; Couvreur, P.; Serre, C. *Angew. Chem., Int. Ed.* **2010**, *49*, 6260−6266. (h) Liu, Y.; Xuan, W. M.; Cui, Y. *Adv. Mater.* **2010**, *22*, 4112−4135.

(5) (a) Yi, F.-Y.; Yang, W. T.; Sun, Z.-M. *J. Mater. Chem.* **2012**, *22*, 23201−23209. (b) Kent, C. A.; Liu, D. M.; Meyer, T. J.; Lin, W. B. *J. Am. Chem. Soc.* **2012**, *134*, 3991−3994. (c) He, Y. B.; Zhou, W.; Krishna, R.; Chen, B. L. *Chem. Commun.* **2012**, *48*, 11813−11831. (d) Zhan, W.-W.; Kuang, Q.; Zhou, J.-Z.; Kong, X.-J.; Xie, Z.-X.; Zheng, L.-S. *J. Am. Chem. Soc.* **2013**, *135*, 1926−1933. (e) Meilikhov, M.; Furukawa, S.; Hirai, K.; Fischer, R. A.; Kitagawa, S. *Angew. Chem., Int. Ed.* **2013**, *52*, 341−345. (f) Sun, C.-Y.; Wang, X.-L.; Qin, C.; Jin, J.-L.; Su, Z.-M.; Huang, P.; Shao, K.-Z. *Chem.—Eur. J.* **2013**, *19*, 3639−3645. (g) Li, Y.-W.; Li, J.-R.; Wang, L.-F.; Zhou, B.-Y.; Chen, Q.; Bu, X.-H. *J. Mater. Chem. A* **2013**, *1*, 495−499. (h) Lü, Y. Y.; Zhan, W. W.; He, Y.; Wang, Y. T.; Kong, X. J.; Kuang, Q.; Xie, Z. X.; Zheng, L. S. *ACS Appl. Mater. Interfaces* **2014**, *6*, 4186−4195. (i) Yoon, S. M.; Warren, S. C.; Grzybowski, B. A. *Angew. Chem., Int. Ed.* **2014**, *53*, 4437−4441.

(6) (a) D'Andrade, B. W.; Forrest, S. R. *Adv. Mater.* **2004**, *16*, 1585−1595. (b) Wang, P.; Ma, J.-P.; Dong, Y.-B.; Huang, R.-Q. *J. Am. Chem. Soc.* **2007**, *129*, 10620−10621. (c) Wang, M.-S.; Guo, S.-P.; Li, Y.; Cai, L.-Z.; Zou, J.-P.; Xu, G.; Zhou, W.-W.; Zheng, F.-K.; Guo, G.-C. *J. Am. Chem. Soc.* **2009**, *131*, 13572−13573. (d) Sun, C.-Y.; Wang, X.-L.; Zhang, X.; Qin, C.; Li, P.; Su, Z.-M.; Zhu, D.- X.; Shan, G.-G.; Shao, K.-Z.; Wu, H.; Li, J. *Nat. Commun.* **2013**, *4*, 2716−2717.

(7) (a) Kent, C. A.; Mehl, B. P.; Ma, L. Q.; Papanikolas, J. M.; Meyer, T. J.; Lin, W. B. *J. Am. Chem. Soc.* **2010**, *132*, 12767−12769. (b) Zhang, X. D.; Ballem, M. A.; Hu, Z.-J.; Bergman, P.; Uvdal, K. *Angew. Chem., Int. Ed.* **2011**, *50*, 5729−5733. (c) Streit, H. C.; Adlung, M.; Shekhah, O.; Stammer, X.; Arslan, H. K.; Zybaylo, O.; Ladnorg, T.; Gliemann, H.; Franzreb, M.; Wöll, C.; Wickleder, C. *ChemPhysChem* **2012**, *13*, 2699−2702. (d) Suresh, V. M.; George, S. J.; Maji, T. K. *Adv. Funct. Mater.* **2013**, *23*, 5585−5590. (e) Sun, L. B.; Xing, H. Z.; Liang, Z. Q.; Yu, J. H.; Xu, R. R. *Chem. Commun.* **2013**, *49*, 11155−11157.

(8) (a) Evans, O. R.; Lin, W. B. *Acc. Chem. Res.* **2002**, *35*, 511−522. (b) Zang, S. Q.; Su, Y.; Li, Y. Z.; Ni, Z. P.; Meng, Q. J. *Inorg. Chem.* **2006**, *45*, 174−180. (c) Yang, J.; Li, G. D.; Cao, J. J.; Yue, Q.; Li, G.-H.; Chen, J. S. *Chem.—Eur. J.* **2007**, *13*, 3248−3261. (d) Wang, C.; Zhang, T.; Lin, W. B. *Chem. Rev.* **2012**, *112*, 1084−1104. (e) Huang, K. X.; Song, Y. L.; Pan, Z. R.; Li, Y. Z.; Zhuo, X.; Zheng, H. G. *Inorg. Chem.* **2007**, *46*, 6233−6235. (f) Xu, C.; Zhang, Z.-Y.; Ren, Z.-G.; Zhou, L.-K.; Li, H.-X.; Wang, H.-F.; Sun, Z.-R.; Lang, J.-P. *Cryst. Growth Des.* **2013**, *13*, 2530−2539. (g) Wei, Z.-H.; Ni, C.-Y.; Li, H.-X.; Ren, Z.-G.; Sun, Z.-R.; Lang, J.-P. *Chem. Commun.* **2013**, *49*, 4836−4838. (h) Zhang, Z.-Y.; Gong, W.-G.; Wang, F.; Chen, M.-M.; Zhou, L.-K.; Ren, Z.-G.; Sun, Z.-R.; Lang, J.-P. *Dalton Trans.* **2013**, *42*, 9495−9504.

(9) (a) Kataoka, Y.; Sato, K.; Miyazaki, Y.; Masuda, K.; Tanaka, H.; Naito, S.; Mori, W. *Energy Environ. Sci.* **2009**, *2*, 397−400. (b) Silva, C. G.; Luz, I.; Xamena, F. X. L. I; Corma, A.; García, H. *Chem.—Eur. J.* **2010**, *16*, 11133−11138. (c) Krafft, K. E.; Wang, C.; Lin, W. B. *Adv. Mater.* **2012**, *24*, 2014−2018. (d) He, J.; Yan, Z. Y.; Wang, J. Q.; Xie, J.; Jiang, L.; Shi, Y. M.; Yuan, F. G.; Yu, F.; Sun, Y. J. *Chem. Commun.* **2013**, *49*, 6761−6763. (e) Fateeva, A.; Chater, P. A.; Ireland, C. P.; Tahir, A. A.; Khimyak, Y. Z.; Wiper, P. V.; Darwent, J. R.; Rosseinsky, M. J. *Angew. Chem., Int. Ed.* **2012**, *51*, 7440−7444. (f) Wang, C.; deKrafft, K. E.; Lin, W. B. *J. Am. Chem. Soc.* **2012**, *134*, 7211−7214. (g) Zhou, T. H.; Du, Y. H.; Borgna, A.; Hong, J. D.; Wang, Y. B.; Han, J. Y.; Zhang, W.; Xu, R. *Energy Environ. Sci.* **2013**, *6*, 3229−3234.

(10) (a) Zhao, B.; Chen, X.-Y.; Cheng, P.; Liao, D.-Z.; Yan, S.-P.; Jiang, Z.-H. *J. Am. Chem. Soc.* **2004**, *126*, 15394−15395. (b) Lee, E. Y.; Jang, S. Y.; Suh, M. P. *J. Am. Chem. Soc.* **2005**, *127*, 6374−6381. (c) Zhu, W.-H.; Wang, Z.-M.; Gao, S. *Inorg. Chem.* **2007**, *46*, 1337−1342. (d) Lu, W.-G.; Jiang, L.; Feng, X.-L.; Lu, T.-B. *Inorg. Chem.* **2009**, *48*, 6997−6999. (e) Harbuzaru, B. V.; Corma, A.; Rey, F.; Jordá, J. L.; Ananias, D.; Carlos, L. D.; Rocha, J. *Angew. Chem., Int. Ed.* **2009**, *48*, 6476−6479. (f) Xie, Z. G.; Ma, L. Q.; deKrafft, K. E.; Jin, A.; Lin, W. B. *J. Am. Chem. Soc.* **2010**, *132*, 922−923. (g) Guo, Z.; Xu, H.; Su, S.; Cai, J.; Dang, S.; Xiang, S.; Qian, G.; Zhang, H.; O'Keeffe, M.; Chen, B. *Chem. Commun.* **2011**, *47*, 5551−5553.

DOI: 10.1021/ic502219y
Inorg. Chem. 2015, 54, 1346−1353

(11) (a) Rieter, W. J.; Taylor, K. M. L.; An, H. Y.; Lin, W. L.; Lin, W. B. *J. Am. Chem. Soc.* **2006**, *128*, 9024−9025. (b) Zhang, P.; Steelant, W.; Kumar, M.; Scholfield, M. *J. Am. Chem. Soc.* **2007**, *129*, 4526−4527. (c) Taylor, K. M. L.; Rieter, W. J.; Lin, W. B. *J. Am. Chem. Soc.* **2008**, *130*, 14358−14359. (d) Rowe, M. D.; Thamm, D. H.; Kraft, S. L.; Boyes, S. G. *Biomacromolecules* **2009**, *10*, 983−993. (e) Huxford, R. C.; Rocca, J. D.; Lin, W. B. *Curr. Opin. Chem. Biol.* **2010**, *14*, 262−268. (f) Jung, S.; Kim, Y.; Kim, S.-J.; Kwon, T.-H.; Huh, S.; Park, S. *Chem. Commun.* **2011**, *47*, 2904−2906.

(12) (a) Binnemans, K. *Chem. Rev.* **2009**, *109*, 4283−4374. (b) Rocha, J.; Carlos, L. D.; Paza, F. A. A.; Ananias, D. *Chem. Soc. Rev.* **2011**, *40*, 926−940. (c) Cui, Y. J.; Yue, Y. F.; Qian, G. D.; Chen, B. L. *Chem. Rev.* **2012**, *112*, 1126−1162. (d) Zhang, W.; Xiong, R.-G. *Chem. Rev.* **2012**, *112*, 1163−1195. (e) Heine, J.; Müller-Buschbaum, K. *Chem. Soc. Rev.* **2013**, *42*, 9232−9242. (f) Meyer, L. V.; Schönfeld, F.; Müller-Buschbaum, K. *Chem. Commun.* **2014**, *50*, 8093−8108. (g) Liu, D.; Ren, Z.-G.; Li, H.-X.; Lang, J.-P.; Li, N.-Y.; Abrahams, B. F. *Angew. Chem., Int. Ed.* **2010**, *49*, 4767−4770. (h) Lang, J.-P.; Xu, Q.-F.; Chen, Z.-N.; Abrahams, B. F. *J. Am. Chem. Soc.* **2003**, *125*, 12682−12683.

(13) (a) Loudet, A.; Burgess, K. *Chem. Rev.* **2007**, *107*, 4891−4932. (b) Ziessel, R.; Ulrich, G.; Harriman, A. *New J. Chem.* **2007**, *31*, 496−501. (c) Ulrich, G.; Ziessel, R.; Harriman, A. *Angew. Chem., Int. Ed.* **2008**, *47*, 1184−1201. (d) Benniston, A. C.; Copley, G. *Phys. Chem. Chem. Phys.* **2009**, *11*, 4124−4131.

(14) (a) Karolin, J.; Johansson, L. B.-A.; Strandberg, L.; Ny, T. *J. Am. Chem. Soc.* **1994**, *116*, 7801−7806. (b) Wan, C.-W.; Burghart, A.; Chen, J.; Bergström, F.; Johansson, L. B.-Å.; Wolford, M. F.; Kim, T. G.; Topp, M. R.; Hochstrasser, R. M.; Burgess, K. *Chem.—Eur. J.* **2003**, *9*, 4430−4441. (c) Yogo, T.; Urano, Y.; Ishitsuka, Y.; Maniwa, F.; Nagano, T. *J. Am. Chem. Soc.* **2005**, *127*, 12162−12163. (d) Baruah, M.; Qin, W. W.; Vallée, R. A. L.; Beljonne, D.; Rohand, T.; Dehaen, W.; Boens, N. *Org. Lett.* **2005**, *7*, 4377−4380. (e) Goud, T. V.; Tutar, A.; Biellmann, J.-F. *Tetrahedron* **2006**, *62*, 5084−5091. (f) Tahtaoui, C.; Thomas, C.; Rohmer, F.; Klotz, P.; Duportail, G.; Mély, Y.; Bonnet, D.; Hibert, M. *J. Org. Chem.* **2007**, *72*, 269−272. (g) Oleynik, P.; Ishihara, Y.; Cosa, G. *J. Am. Chem. Soc.* **2007**, *139*, 1842−1843.

(15) (a) Mikhalyov, I.; Gretskaya, N.; Bergström, F.; Johansson, L. B.-Å. *Phys. Chem. Chem. Phys.* **2002**, *4*, 5663−5670. (b) Liao, Y. Y.; Génot, V.; Méallet-Renault, R.; Vu, T. T.; Audibert, J.-F.; Lemaistre, J.-P.; Clavier, G.; Retailleaub, P.; Pansu, R. B. *Phys. Chem. Chem. Phys.* **2013**, *15*, 3186−3195. (c) Choi, S.; Bouffard, J.; Kim, Y. *Chem. Sci.* **2014**, *5*, 751−755.

(16) (a) Nepomnyashchii, A. B.; Bard, A. J. *Acc. Chem. Res.* **2012**, *45*, 1844−1853. (b) Awuah, S. G.; You, Y. *RSC Adv.* **2012**, *2*, 11169−11183. (c) Boens, N.; Leen, V.; Dehaen, W. *Chem. Soc. Rev.* **2012**, *41*, 1130−1172. (d) Kamkaew, A.; Lim, S. H.; Lee, H. B.; Kiew, L. V.; Chung, L. Y.; Burgess, K. *Chem. Soc. Rev.* **2013**, *42*, 77−88. (e) Culzoni, M. J.; Pẽna, A. M. D. L.; Machuca, A.; Goicoechea, H. C.; Babiano, R. *Anal. Methods* **2013**, *5*, 30−49. (f) Ni, Y.; Wu, J. S. *Org. Biomol. Chem.* **2014**, *12*, 3774−3791.

(17) (a) Yee, M.-c.; Fas, S. C.; Stohlmeyer, M. M.; Wandless, T. J.; Cimprich, K. A. *J. Biol. Chem.* **2005**, *280*, 29053−29059. (b) Hattori, S.; Ohkubo, K.; Urano, Y.; Sunahara, H.; Nagano, T.; Wada, Y.; Tkachenko, N. V.; Lemmetyinen, H.; Fukuzumi, S. *J. Phys. Chem. B* **2005**, *109*, 15368−15375. (c) Yuan, M. J.; Li, Y. L.; Li, J. B.; Li, C. H.; Liu, X. F.; Lv, J.; Xu, J. L.; Liu, H. B.; Wang, S.; Zhu, D. B. *Org. Lett.* **2007**, *9*, 2313−2316. (d) Ziessel, R.; Allen, B. D.; Rewinska, D. B.; Harriman, A. *Chem.—Eur. J.* **2009**, *15*, 7382−7393. (e) Zhang, G. Q.; Palmer, G. M.; Dewhirst, M. W.; Fraser, C. L. *Nat. Mater.* **2009**, *8*, 747−751. (f) Bozdemir, O. A.; Guliyev, R.; Buyukcakir, O.; Selcuk, S.; Kolemen, S.; Gulseren, G.; Nalbantoglu, T.; Boyaci, H.; Akkaya, E. U. *J. Am. Chem. Soc.* **2010**, *132*, 8029−8036. (g) Suk, J.; Omer, K. M.; Bura, T.; Ziessel, R.; Bard, A. J. *J. Phys. Chem. C* **2011**, *115*, 15361−15368. (h) Zhang, X. J.; Xu, Y. F.; Guo, P.; Qian, X. H. *New J. Chem.* **2012**, *36*, 1621−1625.

(18) (a) Nastasi, F.; Puntoriero, F.; Campagna, S.; Olivier, J.-H.; Ziessel, R. *Phys. Chem. Chem. Phys.* **2010**, *12*, 7392−7402. (b) Rosenthal, J.; Lippard, S. J. *J. Am. Chem. Soc.* **2010**, *132*, 5536−5537. (c) Whited, M. T.; Djurovich, P. I.; Roberts, S. T.; Durrell, A. C.; Schlenker, C. W.; Bradforth, S. E.; Thompson, M. E. *J. Am. Chem. Soc.* **2011**, *133*, 88−96. (d) Ryu, J. H.; Eom, Y. K.; Bünzli, J.-C. G.; Kim, H. K. *New J. Chem.* **2012**, *36*, 723−731. (e) Sozmen, F.; Oksal, B. S.; Bozdemir, O. A.; Buyukcakir, O.; Akkaya, E. U. *Org. Lett.* **2012**, *14*, 5286−5289. (f) Zhou, Q.-X.; Lei, W.-H.; Hou, Y.-J.; Chen, Y.-J.; Li, C.; Zhang, B.-W.; Wang, X.-S. *Dalton Trans.* **2013**, *42*, 2786−2791. (g) Bartelmess, J.; Weare, W. W.; Sommer, R. D. *Dalton Trans.* **2013**, *42*, 14883−14891.

(19) (a) Wu, W. H.; Sun, J. F.; Cui, X. N.; Zhao, J. Z. *J. Mater. Chem. C* **2013**, *1*, 4577−4589. (b) Sun, J. F.; Zhong, F. F.; Yi, X. Y.; Zhao, J. Z. *Inorg. Chem.* **2013**, *52*, 6299−6310. (c) Shi, W.-J.; Menting, R.; Ermilov, E. A.; Lo, P.-C.; Röder, B.; Ng, D. K. P. *Chem. Commun.* **2013**, *49*, 5277−5279. (d) Majumdar, P.; Yuan, X. L.; Li, S. F.; Guennic, B. L.; Ma, J.; Zhang, C. S.; Jacquemin, D.; Zhao, J. Z. *J. Mater. Chem. B* **2014**, *2*, 2838−2854. (e) Manton, J. C.; Long, C.; Vos, J. G.; Pryce, M. T. *Phys. Chem. Chem. Phys.* **2014**, *16*, 5229−5236. (f) Bartelmess, J.; Francis, A. J.; Roz, K. A. E.; Castellano, F. N.; Weare, W. W.; Sommer, R. D. *Inorg. Chem.* **2014**, *53*, 4527−4534. (g) Chu, G. M.; Guerrero-Martínez, A.; Fernández, I.; Sierra, M. Á. *Chem.—Eur. J.* **2014**, *20*, 1367−1375.

(20) Neelakandan, P. P.; Jiménez, A.; Nitschke, J. R. *Chem. Sci.* **2014**, *5*, 908−915.

(21) Lee, C. Y.; Farha, O. K.; Hong, B. J.; Sarjeant, A. A.; Nguyen, S. B. T.; Hupp, J. T. *J. Am. Chem. Soc.* **2011**, *133*, 15858−15861.

(22) Zhou, L.; Xue, Y.-S.; Xu, Y.; Zhang, J.; Du, H.-B. *CrystEngComm* **2013**, *15*, 7315−7320.

(23) Komatsu, T.; Urano, Y.; Fujikawa, Y.; Kobayashi, T.; Kojima, H.; Terai, T.; Hanaoka, K.; Nagano, T. *Chem. Commun.* **2009**, 7015−7017.

(24) Sheldrick, G.-M. *Acta Crystallogr., Sect. A* **2008**, *64*, 112−122.

(25) Bergstrom, F.; Mikhalyov, I.; Hagglof, P.; Wortmann, R.; Ny, T.; Johansson, L. B.- A. *J. Am. Chem. Soc.* **2002**, *197*, 196−204.

(26) Vu, T. T.; Dvorko, M.; Schmidt, E. Y.; Audibert, J.-F.; Retailleau, P.; Trofimov, B. A.; Pansu, R. B.; Clavier, G.; Renault, R. M. *J. Phys. Chem. C* **2013**, *117*, 5373−5385.

(27) Vu, T. T.; Badré, S.; Dumas-Verdes, C.; Vachon, J.-J.; Julien, C.; Audebert, P.; Senotrusova, E. Y.; Schmidt, E. Y.; Trofimov, B. A.; Pansu, R. B.; Clavier, G.; Méallet-Renault, R. *J. Phys. Chem. C* **2009**, *113*, 11844−11855.

(28) Liu, B. J.; Wong-Foy, A. G.; Matzger, A. J. *Chem. Commun.* **2013**, *49*, 1419−1421.

DOI: 10.1021/ic502219y
Inorg. Chem. 2015, 54, 1346−1353